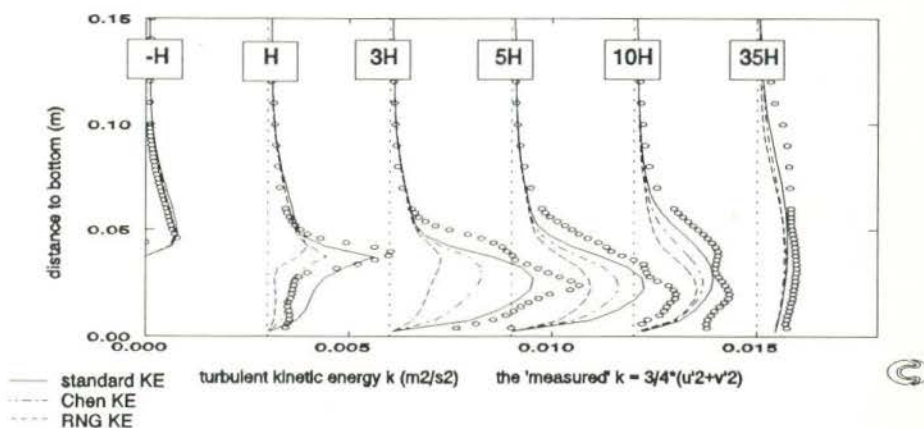


# Calibration of flow model and method to compute particle transport

report 6 of the Rioned project 92-05: research storm water sedimentation tanks

March 1995

Ir. J. Kluck



Values for  $k$  in backward facing step as measured by Tropea and computed with different forms of the  $k$ - $\epsilon$  turbulence model.

# Calibration of flow model and method to compute particle transport

report 6 of the Rioned project 92-05: research storm water sedimentation tanks

March 1995  
ir. J. Kluck  
Sanitary Engineering and Water Management  
Faculty of Civil Engineering  
Delft University of Technology

## TABLE OF CONTENTS

1 INTRODUCTION .....	-1-
2 TURBULENCE MODELLING .....	-2-
2.1 Introduction .....	-2-
2.2 k- $\epsilon$ turbulence model .....	-4-
2.3 Modified forms of the k- $\epsilon$ turbulence model .....	-6-
2.3.1 Chen and Kim modifications of k- $\epsilon$ model .....	-6-
2.3.2 RNG modified k- $\epsilon$ model .....	-7-
2.3.3 Two scale k- $\epsilon$ turbulence model .....	-7-
3 CALIBRATION OF FLOW MODEL .....	-8-
3.1 Flow over a backward facing step .....	-8-
3.1.1 The PHOENICS model .....	-8-
3.1.2 Comparison of the predictions with the measurements ....	-9-
3.1.3 Turbulence level at inflow boundary .....	-12-
3.1.4 Conclusion .....	-13-
3.2 Measured flow in experimental setup .....	-13-
3.2.1 PHOENICS model .....	-13-
3.2.2 Comparison with measurements .....	-15-
3.2.3 Conclusion .....	-15-
3.3 Conclusion flow modelling .....	-15-
4 MODELLING OF SEDIMENTATION .....	-18-
4.1 Particle equilibrium equation .....	-19-
4.2 PHOENICS way of computing .....	-19-
4.3 Implementing sedimentation in PHOENICS .....	-22-
4.4 Simulation of particle distribution during filling of tank .....	-23-
4.4.1 Computations .....	-23-
4.4.2 Particle diffusion .....	-27-
4.4.3 Bottom boundary condition for settleable solids .....	-27-
5 CONTINUATION OF RESEARCH .....	-28-
ANNEXES A: REFERENCES .....	-30-
ANNEXES B: SETTLEABLE SOLIDS SUBROUTINE FOR PHOENICS .....	-31-

# 1 INTRODUCTION

In five reports [*Kluck, 1992-a, 1992-b, 1993-a and 1993-b*] (written in Dutch) and [*Kluck, 1994*] the work which has been done in the period February 1992 to July 1994 is presented. The first report presents the objectives and reason of this research and the existing design methods for storm water sedimentation tanks. In the second report the choice for using PHOENICS to set up a mathematical model is made. Also a start is made with setting up a model for the water movement only. The third report deals with the problems encountered in modelling a varying free surface flow. In the fourth report further progress in modelling the flow of water is presented. In the future the most important parts of these Dutch reports will be translated into English. Finally in the fifth report (in English) the experimental setup is presented, together with a comparison of measurements and predictions with the mathematical model. Also a description of methods to compute the particle distribution influenced by gravity is given.

In this report different forms of the  $k-\epsilon$  turbulence model are presented (Chapter 2). In Chapter 3 the choice for a modified form of the  $k-\epsilon$  turbulence model is made based on the comparison of the predictions and the measurements in the experimental setup and data from literature. In chapter 4 a new method to compute the particle distribution is presented. Finally in chapter 5 the continuation of this research is given.

## 2 TURBULENCE MODELLING

### 2.1 Introduction

In turbulent flow conditions the velocities vary irregularly in time and space. Eddies of different sizes are present and increase the exchange of impulse, heat, solved and suspended matter, etc. In this part the effect of the turbulence on the velocities is discussed.

The computers are not yet powerful enough to simulate a turbulent flow situation by solving the Navier-Stokes equations directly [Kluck 1992-b]. The flow domain would have to be divided into so many cells and the computations would have to be carried out with such small time steps that the simulation becomes impossible. Therefore the turbulence is simplified in a model. Because the time scales at which the turbulent fluctuations take place are much smaller than the times scale at which for example the boundary conditions vary, the exact simulation of the turbulent flow is not necessary. The velocities (and the other turbulent fluctuating variables) can be averaged over a small period. In the momentary (turbulent) velocity an average and a fluctuating component can be discriminated:

$$u(t) = \bar{u} + u'(t)$$

The average velocity is computed over a certain interval  $\Delta t = t_2 - t_1$ .

$$\bar{u} = \frac{1}{\Delta t} \int_{t_1}^{t_2} u(t) dt$$

Combining these two equations gives:

$$\bar{u} = \overline{u(t)} = \overline{u + u'} = \bar{u} + \overline{u'} \quad \text{consequently} \quad \overline{u'} = 0$$

$$\overline{uv} = \bar{u} \bar{v} + \overline{u'v'}$$

and

$$\frac{\partial}{\partial x} (\overline{uv}) = \frac{\partial}{\partial x} (\bar{u} \bar{v}) = \frac{\partial}{\partial x} (\bar{u} \bar{v}) + \frac{\partial}{\partial x} (\overline{u'v'})$$

For incompressible fluids the term  $Du/Dt$  of the Navier-Stokes equation can be written as:

$$\frac{Du}{Dt} = \frac{\partial u}{\partial t} + \frac{\partial uu}{\partial x} + \frac{\partial uv}{\partial y} + \frac{\partial uw}{\partial z}$$

After averaging over a certain interval and splitting the velocity in the average and the fluctuating components only the following terms stay (since the other terms are zero):

$$\frac{D\bar{u}}{Dt} = \frac{\partial \bar{u}}{\partial t} + \bar{u} \frac{\partial \bar{u}}{\partial x} + \bar{v} \frac{\partial \bar{u}}{\partial y} + \bar{w} \frac{\partial \bar{u}}{\partial z} +$$

$$\frac{\partial \overline{u'u'}}{\partial x} + \frac{\partial \overline{u'v'}}{\partial y} + \frac{\partial \overline{u'w'}}{\partial z}$$

The terms on the right hand side on the first line of this equation are the average components. The second line gives the turbulent terms.

To simplify the notation of these equations the bars have been omitted from now on. The characters  $u$ ,  $v$  and  $w$  now represent the averaged velocities (in  $x$ -,  $y$ - and  $z$ -direction respectively). Also the bars on  $u'u'$ ,  $u'v'$ ,  $u'w'$ , etc. have been omitted.

The Navier-Stokes equations averaged over a certain interval are the Reynolds equations. For the  $x$ -direction the Reynolds equation for an incompressible fluid becomes:

$$\frac{Du}{Dt} = -\frac{1}{\rho} \frac{\partial p_x}{\partial x} + \frac{\partial}{\partial x} \left( \nu \frac{\partial u}{\partial x} - u'u' \right) +$$

$$+ \frac{\partial}{\partial y} \left( \nu \frac{\partial u}{\partial y} - u'v' \right) +$$

$$+ \frac{\partial}{\partial z} \left( \nu \frac{\partial u}{\partial z} - u'w' \right) + \frac{1}{\rho} \sum F_{\text{rest}-x}$$

The turbulence creates extra internal stresses, the turbulent or Reynold stresses:

$$\rho u'v' = \text{transport of } x\text{-momentum in } y\text{-direction.}$$

In most turbulent flow situations the Reynold or turbulent stresses are much larger than the laminar stresses  $\rho \nu \partial u / \partial x$  etc. [Rodi, 1980]. For the turbulent flow situation in a storm water sedimentation tank the laminar part can be neglected.

The modelling of the turbulence is in fact a matter of estimating these turbulent stresses. One of the existing methods uses the eddy-viscosity-concept. The Reynold stresses are dealt with in a similar way as the viscous forces, by the introduction of an extra viscosity: the turbulent viscosity  $\nu_t$ . It is assumed that the turbulent stresses are a function of the gradients of the average velocities:

$$-u'u' = 2\nu_t \frac{\partial u}{\partial x} - \frac{2}{3}k$$

$$-u'v' = \nu_t \left( \frac{\partial u}{\partial y} + \frac{\partial v}{\partial x} \right)$$

$$-u'w' = \nu_t \left( \frac{\partial u}{\partial z} + \frac{\partial w}{\partial x} \right)$$

The variable  $k$  represents the turbulent kinetic energy per mass in the flow direction.

$$k = \frac{1}{2}(u'^2 + v'^2 + w'^2)$$

Modelling the turbulence thus means the determination of  $k$  and  $\nu_t$ . However, the turbulent viscosity  $\nu_t$  is not a real property of the fluid like the molecular viscosity, but depends on the turbulence. Many proposals to determine  $k$  and  $\nu_t$  have resulted in a range of turbulence models. In most models a relation between  $\nu_t$  and the size of the eddies and the turbulence is assumed. E.g:

$$\nu_t = C_\nu L \sqrt{k}$$

With  $C_\nu$  = constant for  $\nu_t$  (-),  
 $L$  = length scale (m).

Simple turbulence models with a fixed length scale for the eddies or a length scale derived from simple algebraic equations are expected not to be appropriate for modelling the flow in constructions like storm water sedimentation tanks, because the length scale will vary in time and place in the time varying flow. A model which computes this length scale has to be used. The variable  $k$  is solved in a transport equation as given in the next paragraph.

## 2.2 k-ε turbulence model

The k-ε turbulence model is commonly used for flow situations in which the length scales of the eddies are not easy to estimate. The length scale is determined by assuming a relation between the dissipation of turbulent kinetic energy (from the largest eddies to the small eddies where energy is lost in molecular heat production), the turbulent kinetic energy and the length scale. Consequently the length scale can be omitted from the equations:

$$\nu_t = C_{\mu D} \frac{k^2}{\epsilon}$$

with  $C_{\mu D}$  = constant  $\approx 0,09$  (-),  
 $\epsilon$  = dissipation of turbulent kinetic energy ( $m^2/s^3$ ).

In this way the problem is shifted to solving the values of  $k$  and  $\epsilon$ . Both  $k$  and  $\epsilon$  are obtained from transport equations [Rodi, 1980]:

$$\frac{Dk}{Dt} = \nabla_i \left( \frac{v_t}{\sigma_k} \nabla_i k \right) + v_t \left( (\nabla_i v_j)^2 + (\nabla_i v_j)(\nabla_j v_i) \right) - \epsilon$$

$$\frac{D\epsilon}{Dt} = \nabla_i \left( \frac{v_t}{\sigma_\epsilon} \nabla_i \epsilon \right) + C_{pe} k \left( (\nabla_i v_j)^2 + (\nabla_i v_j)(\nabla_j v_i) \right) - C_{de} \frac{\epsilon^2}{k}$$

As much as 5 constants are used in the  $k$ - $\epsilon$  model ( $C_{\mu D}$ ,  $C_{pe}$ ,  $C_{de}$ ,  $\sigma_k$  en  $\sigma_\epsilon$ ) to ensure that the model is valid for a range of flow conditions. Within PHOENICS these constants have been declared as follows:

$$\begin{aligned} C_{\mu D} &= 0.09 \\ C_{pe} &= 1.44 \\ C_{de} &= 1.92 \\ \sigma_k &= 1.0 \\ \sigma_\epsilon &= 1.314 \end{aligned}$$

The equations for  $k$  and  $\epsilon$  are solved together with the continuity equation and the Reynolds equations for turbulent flow:

$$\begin{aligned} \frac{Du}{Dt} = & - \frac{1}{\rho} \frac{\partial p_x}{\partial x} + \frac{\partial}{\partial x} \left( (v + v_t) \frac{\partial u}{\partial x} - \frac{2}{3} k \right) + \\ & + \frac{\partial}{\partial y} \left( (v + v_t) \frac{\partial u}{\partial y} \right) + \\ & + \frac{\partial}{\partial z} \left( (v + v_t) \frac{\partial u}{\partial z} \right) + \frac{1}{\rho} \sum F_{rest-x} \end{aligned}$$

$$\begin{aligned} \frac{Dv}{Dt} = & - \frac{1}{\rho} \frac{\partial p_y}{\partial y} + \frac{\partial}{\partial y} \left( (v + v_t) \frac{\partial v}{\partial y} - \frac{2}{3} k \right) + \\ & + \frac{\partial}{\partial x} \left( (v + v_t) \frac{\partial v}{\partial x} \right) + \\ & + \frac{\partial}{\partial z} \left( (v + v_t) \frac{\partial v}{\partial z} \right) + \frac{1}{\rho} \sum F_{rest-y} \end{aligned}$$

$$\begin{aligned} \frac{Dw}{Dt} = & - \frac{1}{\rho} \frac{\partial p_z}{\partial z} + \frac{\partial}{\partial z} \left( (v + v_t) \frac{\partial w}{\partial z} - \frac{2}{3} k \right) + \\ & + \frac{\partial}{\partial x} \left( (v + v_t) \frac{\partial w}{\partial x} \right) + \\ & + \frac{\partial}{\partial y} \left( (v + v_t) \frac{\partial w}{\partial y} \right) + \frac{1}{\rho} \sum F_{rest-z} \end{aligned}$$



This reasonable simple way of modelling the turbulence, contains some deficiencies. The  $k$ - $\epsilon$  turbulence model, employs a single time scale ( $k/\epsilon$ ) to characterize the various dynamic processes occurring in turbulent flows. Accordingly, the source, sink and transport terms contained in the closed set of model equations are held to proceed at rates proportional to  $\epsilon/k$ . Turbulence, however, comprises fluctuating motions with a spectrum of time scales, and a single-scale approach is unlikely to be adequate under all circumstances because different turbulence interactions are associated with different parts of the spectrum [CHAM].

Furthermore the standard  $k$ - $\epsilon$  model assumes isotropic turbulent values. It is however likely that the eddies are hindered by the presence of walls and thus that the eddies in a plane parallel to a wall are larger than those in a perpendicular plane.

These deficiencies make that the  $k$ - $\epsilon$  model does not predict a turbulent flow situation perfectly. It is reported that the standard  $k$ - $\epsilon$  model underestimates the length of the recirculation zone. Probably the value of the turbulent viscosity in the mixing layer (on top of the recirculation zone) becomes too high. This results in too much diffusion and thus in a faster damping of differences in velocities. Consequently the computed recirculation zone becomes too short. The turbulent viscosity will be smaller if the value of  $k$  is smaller or if the value of  $\epsilon$  is larger. Some modified forms of the  $k$ - $\epsilon$  turbulence model accomplish this.

Possibly the processes in turbulence are not described well with the  $k$ - $\epsilon$  turbulence model. Consider a turbulent mixing layer like in a flow over a backward facing step. The value of  $k$  as measured with  $k = \frac{1}{2}(u'^2 + v'^2 + w'^2)$  will be high if in the turbulent mixing layer coherent sections of water are moving up and down. The exchange with the surrounding water might however remain relatively low if the water stays together. If this is true the value of  $\nu_t$  is overestimated when computed as  $0.09 k^2/\epsilon$ .

However the  $k$ - $\epsilon$  turbulence model is probably the best working turbulence model, since its validity in many different flow situations is proven and it is widely used.

## 2.3 Modified forms of the $k$ - $\epsilon$ turbulence model

Except for the standard form of the  $k$ - $\epsilon$  turbulence model some modified forms are available within PHOENICS. To improve the outcome of the simulations is investigated whether the modified forms of the turbulence model result in better predictions. All these forms of the  $k$ - $\epsilon$  turbulence model still assume isotropy in turbulence and only try to improve the working by changing the rate of production or dissipation.

### 2.3.1 Chen and Kim modifications of $k$ - $\epsilon$ model

In order to ameliorate the working of the standard model, Chen and Kim [Chen, 1987] proposed a modification which increases the value of  $\epsilon$  when  $du/dy$  or  $dv/dx$  are large by introducing an additional time scale ( $k/P_k$ ), where  $P_k$  is the volumetric production rate of  $k$ . In addition, several of the standard model

coefficients are adjusted so that the model maintains good agreement with experimental data on classical turbulent shear layers:

$$\sigma_k = 0.75; \sigma_\epsilon = 1.15; C_{p\epsilon} = 1.15; C_{d\epsilon} = 1.9.$$

The extra time scale  $k/Pk$  is included in the  $\epsilon$ -equation via the following additional source term per unit volume:

$$S_\epsilon = \rho * 0.25 * Pk^2/k$$

### **2.3.2 RNG modified k- $\epsilon$ model**

Another form of the k- $\epsilon$  model provided within PHOENICS is the Renormalization Group (RNG) k- $\epsilon$  model. In this turbulence model an additional source term decreases the value of  $\epsilon$  for large strains ( $du/dy$  or  $dv/dx$  large). See the PHOENICS manual for further information.

### **2.3.3 Two scale k- $\epsilon$ turbulence model**

In order to obtain a better prediction of the turbulent flow situation the turbulent kinetic energy is split in a production and a transfer part in the two scale split k- $\epsilon$  model. For each part a differential equation is solved. Moreover an extra variable for the dissipation of turbulent kinetic energy from the production to the transfer range (where the energy is dissipated) is solved. More information is given in the PHOENICS manual.

### 3 CALIBRATION OF FLOW MODEL

For the calibration of the PHOENICS flow model measurements from a scale model of a storm water sedimentation tank are available [Kluck, 1994]. Comparison of the predictions of the 2-dimensional mathematical models with the measurements show that the flow is predicted fairly well. However, the computed length of the recirculation zone is shorter than the measured length [Kluck, 1994]. The use of a modified  $k-\epsilon$  turbulence model appeared to improve the computational outcome and resulted in a longer recirculation zone. To investigate the pros and the cons of the different forms of the  $k-\epsilon$  turbulence model (provided within PHOENICS) not only these measurements are used. The flow in the experimental setup appeared to be a 3-dimensional one, which makes it less suitable for calibration purposes. The measurements on a backward facing step carried out by Tropea with a Laser Doppler Anemometer (LDA) [Tropea, 1982] are more suitable and have been used to calibrate the flow model. Finally the results of 3-dimensional flow predictions are compared to the measurements in the experimental setup.

#### 3.1 Flow over a backward facing step

The flow over a backward facing step is much simpler than the flow through a storm water sedimentation tank, but contains two important flow characteristics of the flow in a storm water sedimentation tank: the separating and the reattachment point. The separating point is fixed by the lay-out at either the top of the step or the top of the weir. The location of the reattachment point is undefined in both situations and has to be computed by the model.

Except for the average horizontal and vertical velocities also the turbulent fluctuations have been recorded. These data are used to investigate which form of the  $k-\epsilon$  model should be preferred to predict the flow with PHOENICS.

From [Tropea, 1982] the highly turbulent flow situation with a free water surface (situation II) has been chosen.  $H$ , the height of the step is 4 cm. The total depth is 33 cm. The average inflow velocity is 0.372 m/s. Measurements have only been carried out at the lower 12 cm of the flume. The following variables were measured:

- $u$  = average horizontal velocity in the main flow direction,
- $v$  = average vertical velocity,
- $u'^2$  = turbulent fluctuation of horizontal velocity,
- $v'^2$  = turbulent fluctuation of vertical velocity,
- $u'v'$  = turbulent fluctuation of horizontal and vertical velocity.

##### 3.1.1 The PHOENICS model

The flow situation over a backward facing step is modelled with PHOENICS. The flow domain is divided into  $110 \times 34$  cells (horizontally\*vertically). The left-side border of the flow domain is at 14 cm left of the step. The flow domain stretches for 160 cm after the step, so the total length is 174 cm. See figure 3.1. As upper boundary at 0.33 cm above the bottom level after the step a rigid lid is given.

### Boundary conditions

The inflow is at the left (14 cm before the step) over the full depth. The mass and momentum inflow is declared as measured at  $x = -H$ . The vertical velocity equals zero. The values of  $k$  are computed from the measured turbulent fluctuations of the velocities as  $k = \frac{3}{4}(u'^2 + v'^2)$ . For the values of the dissipation of turbulent kinetic energy the following equation is used [Tropea, 1982]:

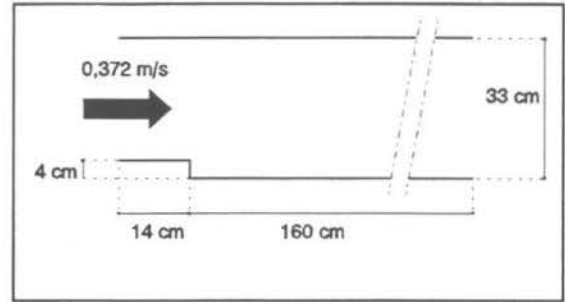


Figure 3.1: Flow over backward facing step.

$$\epsilon = \frac{k^{\frac{3}{2}} C_{\mu D}^{\frac{3}{4}}}{\frac{h}{2} \left( 0.14 - 0.08 \left( 1 - 2 \frac{Y_0}{h} \right)^2 - 0.06 \left( 1 - \frac{Y_0}{h} \right)^4 \right)}$$

The outflow boundary at the right over the full depth is a hydrostatic pressure. The water can flow out freely.

At the bottom the standard PHOENICS wall functions are used (Law of the wall).

As upper boundary a rigid lid is used, with a special boundary condition for  $\epsilon$  to prevent too high turbulence at the free surface [Kluck 1992-b].

Next to the standard  $k-\epsilon$  model some modified forms of the  $k-\epsilon$  model were used to compute the turbulence: Chen, RNG and Two scale, as discussed before.

### 3.1.2 Comparison of the predictions with the measurements

The measured length of the recirculation zone is between  $5 \cdot H$  and  $6 \cdot H$ . The flow fields are in reasonable good agreement with the measurements for all computations with the different forms of the  $k-\epsilon$  turbulence model. See figure 3.2. The model with the standard  $k-\epsilon$  model computes the shortest recirculation zone:  $4.3 \cdot H$ , which is shorter than the measured length. The model with the RNG  $k-\epsilon$  version gives too long a recirculation zone:  $8.2 \cdot H$ . The Chen modification resulted in a length of  $5.4 \cdot H$ .

Just behind the step the velocities of the RNG model fit the measurements best. After the recirculation zone the velocities computed with the standard  $k-\epsilon$  model are closest to the measurements, but there the differences in velocities as computed with the different models are negligible. The Chen modifications result in intermediate values.

The use of the Two scale  $k-\epsilon$  model did not improve the predictions. The values of the horizontal velocity are in between those of the standard and the Chen modified  $k-\epsilon$  models.

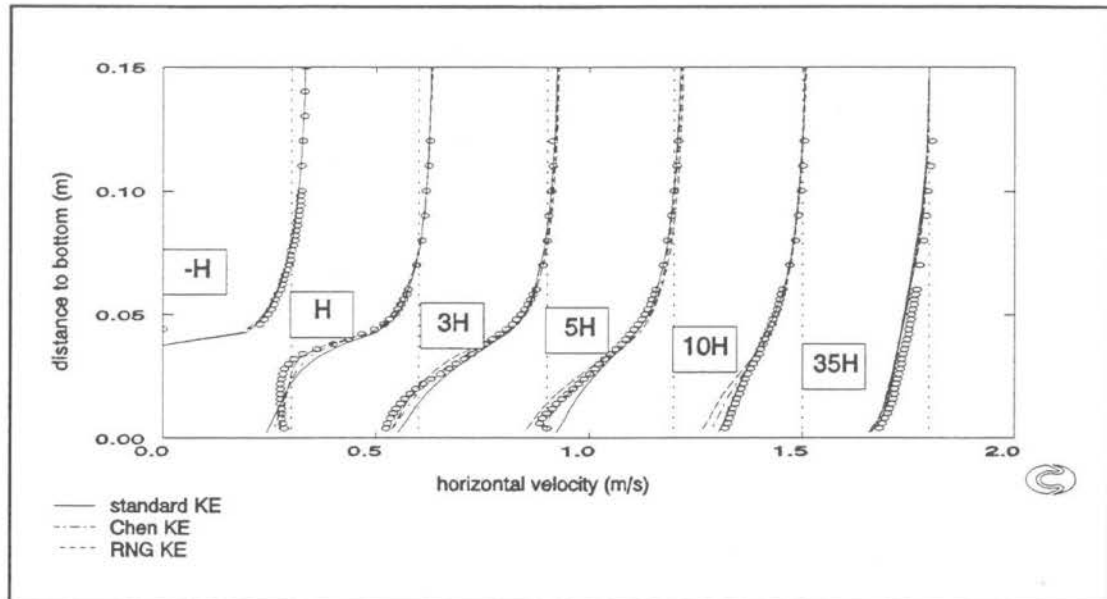


Figure 3.2: Horizontal velocities in a flow over a backward facing step as measured by Tropea and computed with different forms of the  $k$ - $\epsilon$  turbulence model.

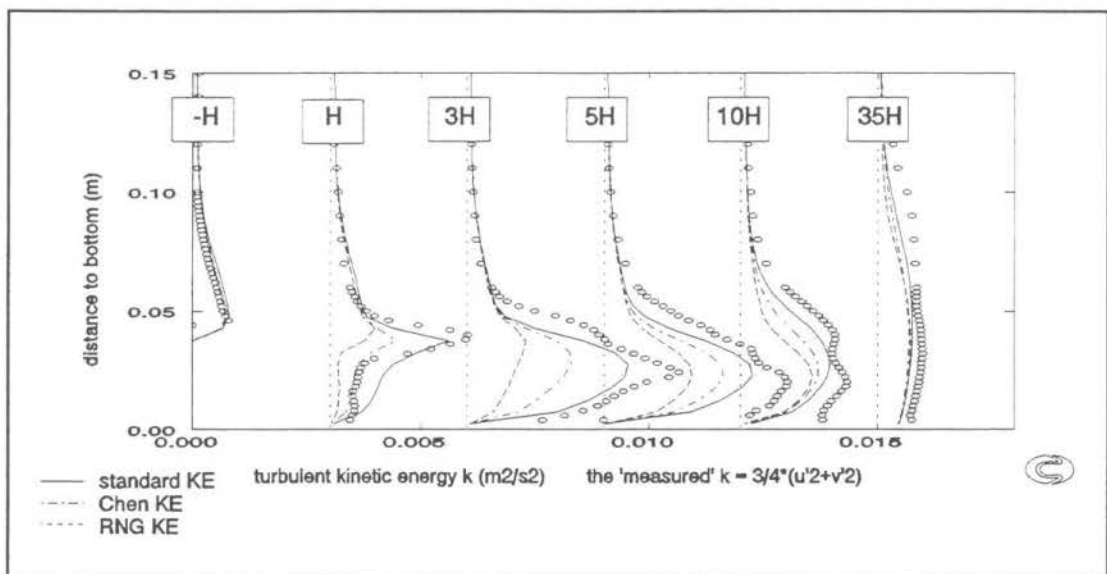


Figure 3.3: Values for  $k$  in backward facing step as measured by Tropea and computed with different forms of the  $k$ - $\epsilon$  turbulence model.

Based on the velocities and the length of the recirculation zone, the model with the Chen modifications can be selected as the most suitable form of the  $k$ - $\epsilon$  model. Before this choice is made the values of the turbulent kinetic energy are investigated. In figure 3.3 the computed values of the turbulent kinetic energy  $k$  are plotted together with the measured values. The measured values have been derived from the turbulent fluctuations of the velocities. In a 3-D situation the value of  $k$  is:

$$k = \frac{1}{2}(u'^2 + v'^2 + w'^2).$$

Because the value of  $w'^2$  has not been measured the value of  $w'^2$  is assumed to be equal to  $1/2(u'^2 + v'^2)$  [Tropea, 1982]. This results in<sup>1</sup>

$$k = 3/4(u'^2 + v'^2)$$

Figure 3.4 shows important differences in the values for  $k$  computed with the three different forms of the  $k-\epsilon$  model. The  $k$  values computed with the standard  $k-\epsilon$  model are the highest, the  $k$  values of the RNG model the smallest. The Chen model results in intermediate values. The values of  $k$  as computed with the Two scale  $k-\epsilon$  model are smaller than those computed with the Chen model. The peaks of the measured values are always higher.

The big differences in  $k$  values in the recirculation zone give reasons to doubt the functioning of the turbulence model. A closer look is needed. The measure for the length of the turbulent vortexes is  $L = k^{3/2}/\epsilon$ . The value of  $L$  appeared to be within reasonable ranges for all three models. At 0.15 m from the bottom and higher  $L$  equals about 0.11 m for all models. In the recirculation zone the standard  $k-\epsilon$  model results in a peak of 4 cm, which grows to 7.5 cm at  $x = 25 \cdot H$ . The RNG model computes a smaller peak in the recirculation zone (3 cm), and only 6.5 cm at  $x = 25 \cdot H$ . The Chen model results in intermediate values.

Another variable to study is the turbulent viscosity  $\nu_t$ . The value of  $\nu_t$  is important, because it is used to compute the diffusion of momentum and suspended matter by turbulence. From the measurements  $\nu_t$  is computed as a function of the turbulent fluctuations of the velocities and the average velocity gradients:

$$\nu_t = \frac{-\overline{u'v'}}{\frac{du}{dy} + \frac{dv}{dx}}$$

The results are given in figures 3.4 and 3.5. The lines composed of the measurements show large fluctuations. These fluctuations are due to the way these values have been computed:  $dx$  is much larger than  $dy$ , and the recorded accuracy of  $u$  and  $v$  is only 0.01 m/s, which is not enough to compute  $du$  and  $dv$  accurately.

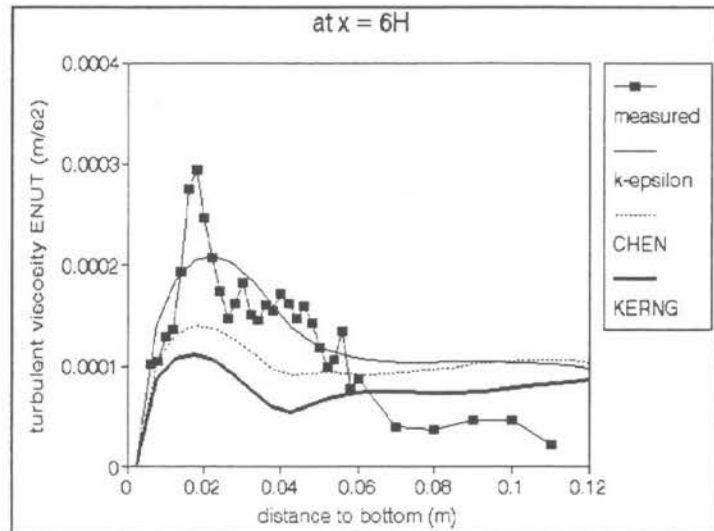


Figure 3.4: Measured and computed  $\nu_t$  at  $x = 6 \cdot H$  in backward facing step.

<sup>1</sup> According to [Nezu, 1993]:  $u'u'/(2k) = 0.55$ ,  $v'v'/(2k) = 0.17$ ,  $w'w'/(2k) = 0.28$ , so  $w'w' = (u'u' + v'v')/2.6$  which is almost equal to  $3/4(u'u' + v'v')$ .

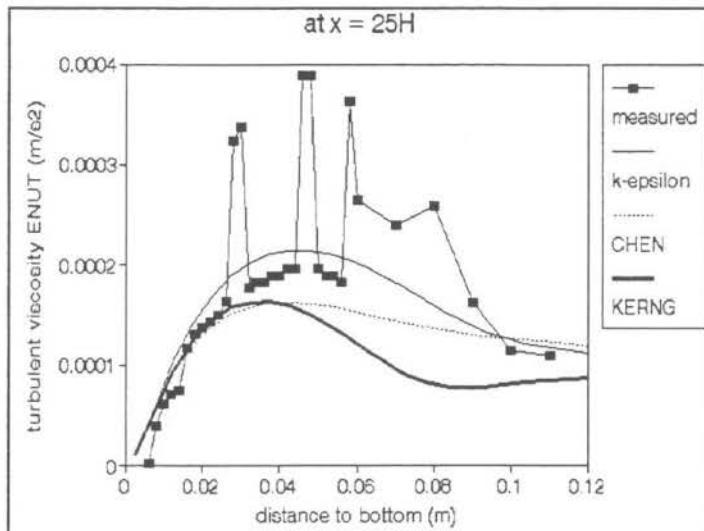


Figure 3.5: Measured and computed  $\nu_t$  at  $x = 25 \cdot H$  in backward facing step.

The standard  $k-\epsilon$  model fits the measurements best. But also the model with the Chen modifications show reasonable results. The RNG model gives clearly too low values for the turbulent viscosity in the recirculation zone.

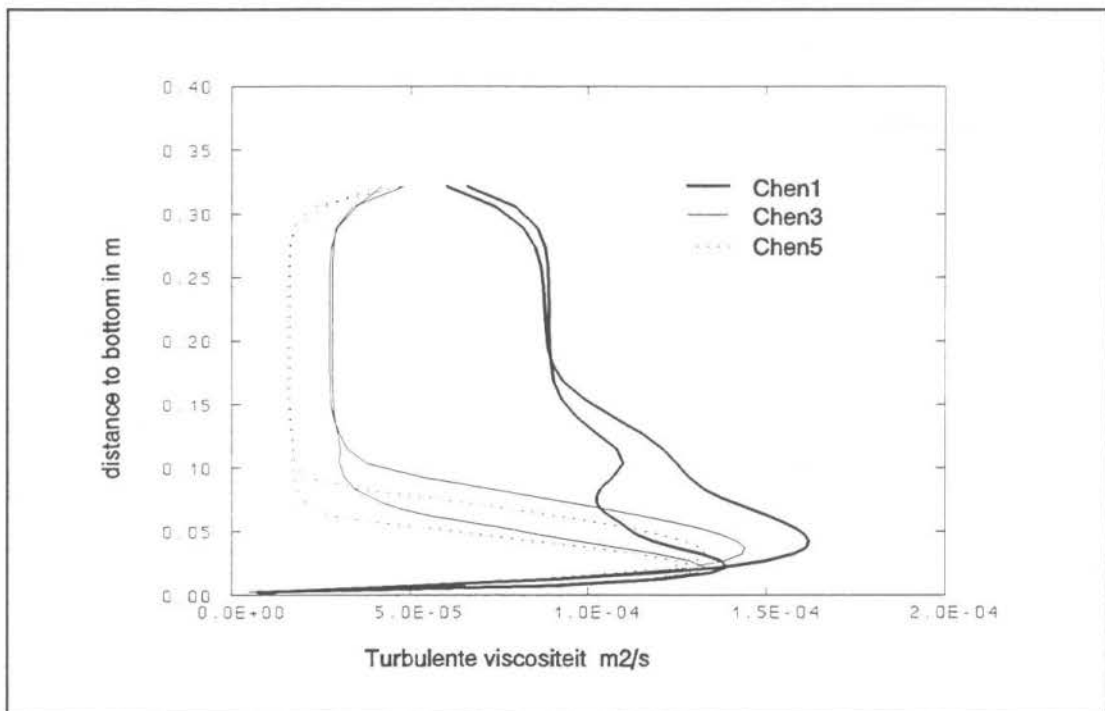


Figure 3.6: Effect of inflow values of  $\epsilon$  on turbulent viscosity levels after the weir.

### 3.1.3 Turbulence level at inflow boundary

The boundary condition for  $\epsilon$  at the inflow appear to determine the value of the turbulence after the recirculation zone. The velocities are hardly influenced by these values as most of the turbulence is generated in the mixing layer. Computations with higher values of  $\epsilon$  at the inflow with the same (measured) values of  $k$  resulted in much lower values of  $\nu_t$  after the recirculation zone. See figure 3.6 in which the values of  $\nu_t$  after the recirculation zone (at  $x = 10 \cdot H$



and  $x = 25 \cdot H$ ) are given for the boundary condition of  $\epsilon$  given in this text (Chen1) and for a 3 times and 5 times larger value  $\epsilon$  (Chen3 and Chen5). For the velocity distribution this does not seem to be important, as the velocity differences in that part of the flow domain are already small. But for the distribution of the suspended solids a correct value of the turbulent viscosity will be important, since this will determine the diffusion.

Since no data is available for the velocities at more than 12 cm from the bottom, the values of  $\nu_t$  could not be derived from the measurements. However, from figure 3.5 is estimated that the turbulent viscosity at 15 to 30 cm from the bottom at  $25 \cdot H$  from the step will be about  $1 \cdot 10^{-4} \text{ m}^2/\text{s}$ . So the boundary condition for  $\epsilon$  as in Chen1 (equation of paragraph 3.1.1) is chosen.

#### 3.1.4 Conclusion

The Chen  $k-\epsilon$  model appears to fit the measurements best and is chosen here. The computational time with this form of the  $k-\epsilon$  turbulence model appeared to be not longer than with the standard  $k-\epsilon$  model.

### 3.2 Measured flow in experimental setup

The measurements in the experimental setup are less accurate than those of [Tropea, 1982], but can be used to validate the 3-D computations. Some computations in 3 dimensions have been presented in [Kluck, 1994]. In the present report the modelling is improved by adding the  $\epsilon$  boundary condition at the water surface, as described in [Kluck, 1993-b]. Furthermore some checks have been carried out. The flow rate in the third situation is 30 l/s. The first and second weir are 14 and 17 cm high. The experimental setup was 1.028 m wide and 4.546 m long. The water level after the first weir was at 22.7 cm from the bottom.

#### 3.2.1 PHOENICS model

For the computations it is important to decide which direction will be the  $z$ -direction since PHOENICS treats the  $z$ -direction different from the  $x$ - and  $y$ -direction. With  $NZ$  is the number of cells in  $z$ -direction, the flow domain is divided in  $NZ$  slabs or  $x-z$  planes. For a certain  $x-z$  plane all the equilibrium equations are solved, before control is governed to the following plane. Iteratively the whole flow domain is solved until the errors are small enough, or the maximum number of iterations has been reached.

Because of this it is advantageous to choose the  $z$ -direction in such a way that in case that the flow has a dominating 2-dimensional flow structure, this 2-dimensional structure is in the  $x-y$  plane. Consequently the iterations in  $z$ -direction will be less important. The flow in the experimental setup is 3-dimensional, but the main circulations are in the vertical plane in the flow direction. Therefore the  $z$ -direction has been chosen as horizontal perpendicular to the main flow direction. In the computations the  $x$ -direction has been chosen as the main flow direction. The  $y$ -direction is used for the vertical direction.

The computational flow domain describes only half (of the width) of the tank, and is divided into  $58 \cdot 8 \cdot 8$  cells ( $x-y-z$ ). For all walls friction was computed. In about 440 sec 1000 sweeps (series of iterations over the whole flow domain) convergence was reached.



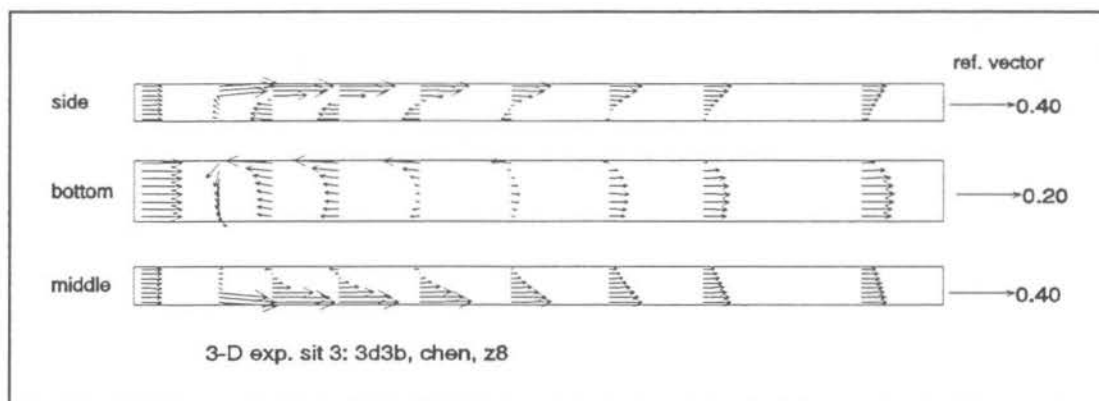


Figure 3.7: Top view of 3-D flow vectors in experimental setup as computed with a coarse grid and the Chen model.

The computations show a clear 3-dimensional flow situation. This flow is induced by the friction at the side wall, bottom and weirs. In figure 3.7 the flow in the experimental setup as computed with a coarse grid and the Chen  $k-\epsilon$  turbulence model is visualized from above. The vectors at the bottom are plotted twice as big as those in the middle and the side. The vectors of the middle plane are presented upside down. The 3-dimensional flow situation appears to be less pronounced than as presented in the former report, but is still very clear. The length of the recirculation zone is shorter in the middle of the tank than at the sides.

To make sure that the resulting 3-D flow was not the result of computational errors, the following tests have been carried out.

- \* Model without friction at sidewall. This resulted in a 2-D flow.
- \* Mirroring of the model in the z-plane: Wall friction at  $IY = NY$ . The result was mirrored (as expected).
- \* Model of total tank instead of a half tank. The results were almost equal to those of the two half tanks.

Consequently the 3-dimensional flow appeared not to be induced by the way of computing.

To check the grid independence of the result a model with a finer grid has been set up: In z-direction 15 cells of 0.033 cm were chosen and in horizontal and vertical direction the flow domain was divided into more sections. This resulted in  $136 \times 12 \times 15$  cells. The velocities computed with the model with the fine grid differ only slightly from those computed with model with the coarse grid, so the coarse grid is fine enough<sup>2</sup>. See figure 3.8 where for the vertical x-plane (perpendicular to the main flow direction) at 120 cm after the weir the horizontal velocities at 10% 25% and 50% of the width are given for a coarse and a fine grid.

<sup>2</sup> or both grids were not fine enough...

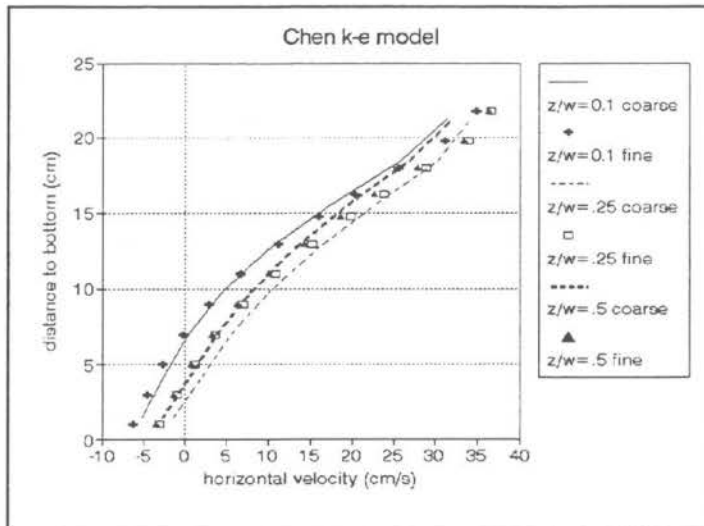


Figure 3.8: Horizontal velocity at  $x = 120$  cm for a coarse and a fine grid.

### 3.2.2 Comparison with measurements

Outside the center plane of the experimental setup too little measurements are available and the results are too scattered to draw firm conclusions. Compared with the measurements the computed flow in the recirculation zone is too smooth: the vertical gradients of the horizontal velocities as computed with the coarse grid and the Chen model are smaller than measured. See figure 3.9 where at 60 cm after weir the computed and measured horizontal velocities are given. However at 120 and 160 cm after the weir, the computations result into larger gradients than the measurements (also figure 3.9).

### 3.2.3 Conclusion

The 3-D modelling of the flow in the tank resulted in somewhat different horizontal velocities in the middle of the width than the width averaged 2-D model. Like in the 2-D model of situation 5 [Kluck, 1994] the 3-D computations with the Chen model result in better resemblance with the measurements just after the weir, but in worse predictions after the recirculation zone. The measurements are too scarce to draw firm conclusions on the correctness of the computed 3-D flow. The clear 3-D flow in the computations is not so clear in the measurements. The velocities can be predicted fairly well. The turbulence variables have not been validated in this flow field.

## 3.3 Conclusion flow modelling

The flow in the experimental setup can be predicted fairly well. The measurements are however not suitable to draw firm conclusions. More accurate validation is carried out with the measurements over a backward facing step. This flow is predicted well with the Chen  $k-\epsilon$  turbulence model. This turbulence model performs better than the standard  $k-\epsilon$  turbulence model and is chosen for the coming computations.

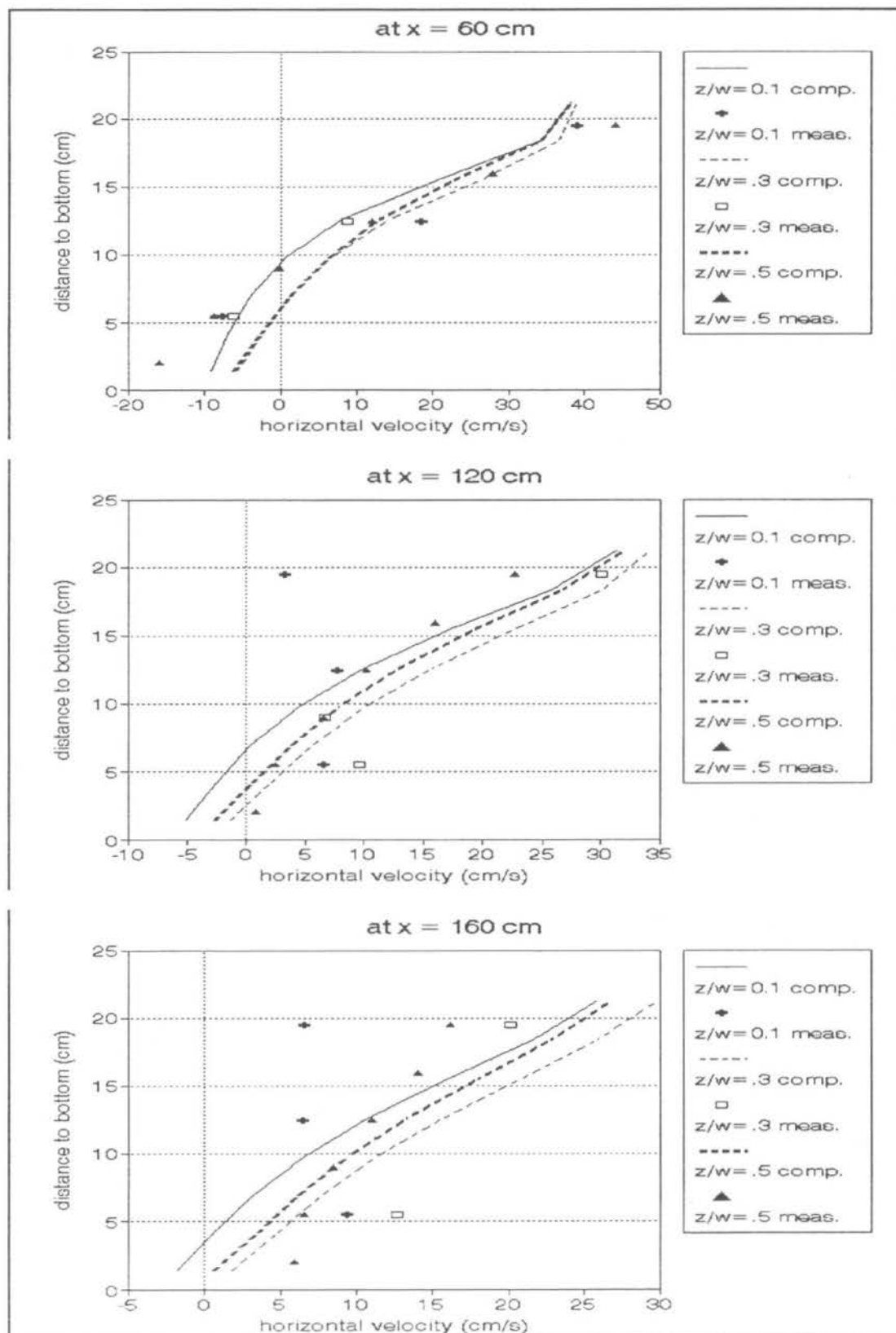


Figure 3.9: Comparison of computations (Chen model and coarse grid) of situation 3 with measurements.

It is expected (and hoped for) that the mathematical modelling of the flow in a real storm water sedimentation tank can be predicted as well as these validated flow situations. This expectation is based upon the fact that the mathematical model consists of generally applicable equilibrium equations. PHOENICS is widely used and tested for all kind of flow situations. Furthermore to obtain good resemblance with the measurements in these computations only a few flow parameters and modelling options have been changed: turbulence model, grid size and level of  $k$  and  $\epsilon$  at the inflow.

The process of setting up the modelling of the flow is consequently stopped and the main future work will be the modelling of the particle transport.

## 4 MODELLING OF SEDIMENTATION

In chapter 5 of [Kluck, 1994] some methods to compute the particle distribution influenced by gravity have been presented. Because the method which was provided with PHOENICS (ASM-method) appeared to neglect the effect of diffusion and is expected to conflict with the method for computing the free surface, an other method was developed. However, this own-written method was not correct, since the discretisation was not fully upwind.

The error which is made in that method can be large compared to the convective mixture transport. In the worst case the sum of the vertical mixture velocity and the slip velocity is zero. Consider for example a 1-dimensional situation consisting of 3 equal cells on top of each other, with an upward velocity equal to the downward slip velocity. The concentration of the middle cell (cell 2) can be computed as a function of the fluxes to and from the cell above (cell 1) and the cell below (cell 3). With the diffusion terms switched off) the following equation is solved:

$$\frac{VOL}{\Delta t}(\rho'c' - \rho c_2) + \rho A v_s (c_1 - c_2) + \rho A v (c_3 - c_2) = 0$$

with  $v$  is the vertical mixture velocity,  $v_s$  is the slip velocity,  $VOL$  is the volume of the cell,  $A$  the area perpendicular to  $v$ ,  $\Delta t$  the time step and  $c'$  and  $\rho'$  respectively the concentration and the density at the old time step. This can be rewritten as:

$$c_2 = \frac{\frac{VOL}{\Delta t} \rho' c' + \rho A v_s c_1 + \rho A v c_3}{\frac{VOL}{\Delta t} \rho + \rho A v_s + \rho A v}$$

In this method the concentration of cell 2 depends on the concentrations in the other cells. It is clear that in this situation without diffusion the concentration of cell 2 should be independent of that in the cells above and below, since  $(v + v_s = 0)$ . The correct way to compute the particle flux has to be based on the final particle velocity, which is the sum of the  $v$  and  $v_s$ . The upwind direction of  $v + v_s$  has to be determined before the flux is computed. This gives:

$$c_2 = \frac{\frac{VOL}{\Delta t} \rho' c' + \max(0, \rho A (v - v_s) c_3) + \max(0, \rho A (v_s - v) c_1)}{\frac{VOL}{\Delta t} \rho + |v_s - v| \rho A}$$

For incompressible fluids this will reduce to  $c_2 = c'$ , which is right in this example.

To accomplish this a new fully upwind method has been set up. The new method has to be used in combination with the Height Of Liquid method of PHOENICS (HOL-method) which is used to simulate a free water surface [Kluck 1993-a]. For the process of setting up the sedimentation equations the diffusion has been switched off. Later the diffusion terms have to be added.

#### 4.1 Particle equilibrium equation

Due to the gravity the particles have a vertical velocity relative to the mixture velocity; the slip velocity. To compute the vertical convective fluxes of particles first the upwind direction for the particles has to be determined. This is not always the same as the upwind direction of the mixture fluid, but is based on the sum of the mixture velocity and the slip velocity.

The particle concentration as used in PHOENICS is dimensionless. The total mass of particles in a cell will be  $\rho * c * V$ . In literature usually the concentration is defined in  $\text{kg/m}^3$ , which is more convenient. Because of the way in which in PHOENICS the scalar variables are computed the concentrations could not be defined in  $\text{kg/m}^3$ , in combination with the HOL-method.

The equilibrium of the concentration in 2 dimensions is:

$$\frac{dc\rho}{dt} + \frac{duc\rho}{dx} + \frac{d(v+v_s)c\rho}{dy} = 0$$

Fully upwind discretisation of this equation gives:

$$\frac{c' \rho' \Delta x \Delta y' - c \rho \Delta x \Delta y}{\Delta T} + u_+ c_{+x} \rho_{+x} \Delta y_+ - u c \rho \Delta y + (v+v_s)_+ c_{+y} \rho_{+y} \Delta x_+ - (v+v_s) c \rho \Delta x = 0$$

or

$$c = \frac{c' \rho' \frac{\Delta x \Delta y}{\Delta T} + u_+ c_{+x} \rho_{+x} \Delta y_+ + (v+v_s)_+ c_{+y} \rho_{+y} \Delta x_+}{\rho \frac{\Delta x \Delta y}{\Delta T} + u \rho \Delta y + (v+v_s) \rho \Delta x}$$

The subscript + indicates the upwind value of a variable.

The addition of x or y indicates the direction.

The ' indicates the variables value of the old time step.

The volume and the cell measures have been taken constant in time.

Computations with this equation resulted in probable particle distributions.

In computations with a free water surface (using the PHOENICS HOL-method), this equation could not be solved in the standard way of PHOENICS, because the simultaneous computation of a free water surface and the particle settling caused serious problems. To explain this first the PHOENICS standard way of computing the distribution of a scalar is presented.

#### 4.2 PHOENICS way of computing

To compute the distribution of a soluble (the transport due to the gravity will be implemented later) the following equations are solved. For the process of setting up the sedimentation equations the diffusion has been switched off.

Consequently in this example the concentration is determined by the convective transport and a time dependent term only.

The fully upwind discretisation is used. For a scalar variable, like a soluble concentration  $c$ , this results for a 2-dimensional case in the following equation:

$$(c'_T - c\rho) \frac{\Delta x \Delta y}{\Delta T} + u_+ c_{+x} \rho_{+x} \Delta y_+ - u c \rho \Delta y + v_+ c_{+y} \rho_{+y} \Delta x_+ - v c \rho \Delta x = 0$$

this can be rewritten as:

$$c = \frac{c'_T \rho \frac{\Delta x \Delta y}{\Delta T} + u_+ c_{+x} \rho_{+x} \Delta y_+ + v_+ c_{+y} \rho_{+y} \Delta x_+}{\rho \frac{\Delta x \Delta y}{\Delta T} + u \rho \Delta y + v \rho \Delta x}$$

Before being solved in PHOENICS, the scalar equilibrium equation is rewritten by substitution of fully upwind form of the equilibrium equation for the fluid:

$$(\rho'_T - \rho) \frac{\Delta x \Delta y}{\Delta T} + u_+ \rho_{+x} \Delta y_+ - u \rho \Delta y + v_+ \rho_{+y} \Delta x_+ - v \rho \Delta x = 0$$

By multiplying this equation by  $c$  and subtracting it from the fully upwind equilibrium equation for the scalars the following equation can be derived:

$$(c'_T - c) \frac{\Delta x \Delta y \rho'_T}{\Delta T} + u_+ (c_{+x} - c) \rho_{+x} \Delta y_+ + v_+ (c_{+y} - c) \rho_{+y} \Delta x_+ = 0$$

The result is that the balance solved is based on the upwind inflowing values of the coefficients multiplied with the concentration differences of the upwind and the current cell:

$$c = \frac{c'_T a_T + c_{+x} a_x + c_{+y} a_y}{a_T + a_x + a_y}$$

with

$$\begin{aligned} a_T &= \Delta x \Delta y \rho'_T / \Delta t = \text{time coefficient;} \\ a_x &= \rho_+ \Delta y_+ u_+; \\ &= \text{coefficient of inflow from the upwind cell in x direction;} \\ a_y &= \rho_+ \Delta x_+ v_+; \\ &= \text{coefficient of inflow from the upwind cell in y direction;} \end{aligned}$$

All inflowing fluxes are taken into account. It is possible that the fluxes are directed inwards from both sides.

In PHOENICS the velocities are computed at the cell faces. All the other variables are computed at the cell centres.

This last equilibrium equation is solved if the standard PHOENICS way of computing the convective fluxes is used. However, in combination with the

HOL-method this last equation appeared not to be equal to the equation without the substitution. This is due to the special way in which the velocities are computed when using the HOL-method. In the HOL method the continuity equation of the fluid is based on the volume fluxes, even though the density is not constant (water surface!). This means that the sum of the densities multiplied by the velocities and the appropriate cell faces is not zero:

$$(\rho' - \rho) \frac{\Delta x \Delta y}{\Delta T} + u_+ \rho_+ \Delta y_+ - u \rho \Delta y + v_+ \rho_+ \Delta x_+ - v \rho \Delta x \neq 0$$

but that for each cell the sum of the horizontal and vertical velocities multiplied by the appropriate cell faces equals zero:

$$u_+ \Delta y_+ - u \Delta y + v_+ \Delta x_+ - v \Delta x = 0$$

The mass equilibrium of the liquid is based on the volume. If the density is not constant (at the water surface) the substitution can not be made. Consequently, the standard PHOENICS way of solving the scalars equilibrium equations is not correct if the HOL-method is used.

To check this problem a simple test case was set up. The flow in a partially filled box was simulated for 1 time step of 0.1 sec. No inflow or outflow takes place. Initially the water is not moving and the water level has a step, so the water starts flowing. The concentration in the water equals 1.0 and in the air the concentration is 0.0. It was expected that using the PHOENICS standard way of computing the concentration would result in an error in the particle mass balance. It appeared however that after one time step the total amount of  $c$  in the flow domain ( $\sum(\rho * c * \text{Volume})$ ) is still almost equal to the initial amount:

$$\begin{aligned} \sum(\rho * c * V) \text{ begin} &= 163.28 \text{ kg;} \\ \sum(\rho * c * V) \text{ after one time step} &= 163.31 \text{ kg.} \end{aligned}$$

Thus, although the cell density is not everywhere equal to the density of the upwind cell, the total mass in the total flow domain stays virtually the same. This might be proven by substituting the equilibrium equation for the water which is solved in the HOL method. According to this equation the change of total amount of liquid in a column of cells is equal to the sum of the in- and out flowing water fluxes. To register the water level the variable VFOL is used, which stands for the volume fraction of liquid of a cell. Its value is 1 if the cell is filled with water only and 0 if it contains only air. At the border of water and air in each column a cell will be partially filled.

$$\text{for each column: } \sum_{IY=1}^{IY=NY} (u_{in} VFOL_{in} \Delta y_+ + u_{out} VFOL_{out} \Delta y + VFOL \Delta y \Delta x) = 0$$

The equality could however not be proven by substituting this equation. In a different test case the error was bigger, and grew every time step. Therefore it was decided not to use the PHOENICS standard way of solving the scalar equations in combination with the HOL method.



### 4.3 Implementing sedimentation in PHOENICS

To solve equation for  $c$  (as given in paragraph 4.1) within PHOENICS the fluxes in vertical direction have to be adjusted to the final particle velocity. Therefore the standard way of computing the convective fluxes has been switched off and the new convective transport is computed together with the sedimentation fluxes in FORTRAN coding written for this purpose. Because of the problem in combination with the HOL method the standard PHOENICS way of computing the concentration has been abandoned and the equilibrium equation of  $c$  (paragraph 4.1) is solved directly.

Because in the HOL-method the water and air are considered as one fluid, a part of the particles moved into the air, which is physically nonsense. This was solved by multiplying the vertical downward fluxes with a factor  $FF$ , and by making the slip velocity dependent on the local fluid density and kinematic viscosity. Consequently, particles which move into these cells drop to the cells below (which will be filled with water).

The equilibrium equation solved is the following:

$$c = \frac{c' \rho' \frac{\Delta x \Delta y}{\Delta T} + u_x c_{x,x} \rho_{x,x} \Delta y + FF(v + v_s)_x c_{x,y} \rho_{x,y} \Delta x}{\rho \frac{\Delta x \Delta y}{\Delta T} + u \rho \Delta y + FF(v + v_s) \rho \Delta x}$$

If the flow is directed downwards the value of  $FF = 1/(\max(0.1, VFOL_{\text{cell above}}))$ . In all other cases  $FF$  equals unity. Thus the flow from a cell which is only partly filled with water, to the cell below is increased. This is done because the lower part of this partly filled cell contains the water with the particles.

The value of the slip velocity  $v_s$  depends on the local fluid density. In air the slip velocity is much higher than in water. To prevent the presence of particles in the air at first the slip velocity was computed as:

$$v_s = -g \frac{\rho_s - \rho_m}{\rho_m} \frac{d^2}{18\nu_m}$$

With

- $\rho_s$  = density of particles,
- $\rho_m$  = density of mixture,
- $\nu_m$  = kinematic viscosity of mixture,
- $d$  = diameter of particles.

This still resulted in too much particles in the air. Therefore the slip velocities in the air have been increased by the introduction of an factor:

$$v_s = -g \frac{\rho_s - \rho_m}{\rho_m} \frac{d^2}{18\nu_m} \left(1 + \frac{\rho_w - \rho_m}{10}\right)$$

Since the density of the mixture has not been made dependent on the particle concentration, the multiplying term is equal to 1 in the water and about 100 in the air.

The equilibrium equation is solved at the end of each time step, which should be no problem because the velocity and other flow variables are assumed to be independent of the particle concentration. When in the future density currents are to be simulated the coding can easily be adapted in such a way that the particle concentration is computed every or every second iteration and the velocities can adapt to the particle concentration.

Computations with this coding resulted in negligible particles concentrations in the air. The particle balance appeared to be correct. Also the flow of water (and particles) over a weir, with a lower water level at the downstream side and consequently the filling of this side, gave good results.

In annexes B the FORTRAN coding used is given.

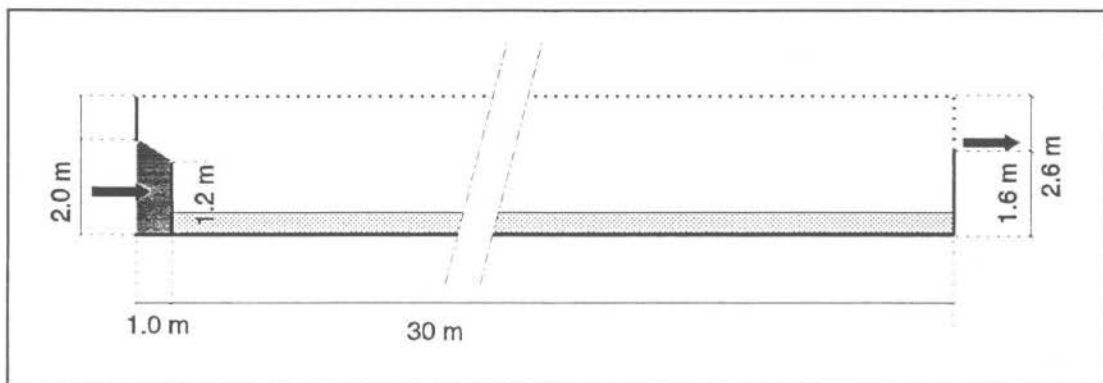
#### 4.4 Simulation of particle distribution during filling of tank

The distribution of particles during the filling of and consequent overflowing out of a rectangular tank has been computed, using the described method.

##### 4.4.1 Computations

The following model has been set up (see also figure 4.1):

Tank of $20 \times 2.6 \text{ m}^2$ divided in $80 \times 13$ cells:	$DX = 0.25 \text{ m}$
	$DY = 0.20 \text{ m}$
The inflow left is uniform over the height $H_{in}$	$H_{in} = 2.0 \text{ m}$
constant horizontal inflow velocity	$u_{in} = 0.05 \text{ m/s}$
so	$q = 0.1 \text{ m}^3/\text{sm}$
surface loading of the tank	$s_o = 0.005 \text{ m/s} = 18 \text{ m/h}$
Height internal weir	$H_i = 1.2 \text{ m}$
Height external weir	$H_e = 1.6 \text{ m}$



Figuur 4.1: Initial situation for filling tank with water with particles

Although the distribution of a range of particles could be evaluated, this has only been done for round particles with a diameter of  $0.0001 \text{ m}$  and a density of  $2650 \text{ kg/m}^3$ . The (constant) slip velocity of such particles is  $0.005025 \text{ m/s}$ . It is assumed that the settling of particles is not hindered by the presence of other particles.

$$v_s = 1.65 * g * d^2 / (18 \nu)$$

$$v_s = 0.005025 \text{ m/s}$$

$$d = 0.0001 \text{ m}$$

$$\rho_s = 2650 \text{ kg/m}^3$$

Inflow concentration settleable particles

$$St_{in} = 1 \text{ (dimensionless)}$$

Initially the tank is filled with 0.4 m clear water (2 rows of cells), to speed up the computations. Above the water in the model is air. In figure 4.2 the situation at 10, 60, 180 and 300 seconds is given. In figure 4.3 the situation at 420, 600 and 780 seconds is given. The water enters the flow domain at the left, flows over the internal weir and fills the tank with water (containing the particles). The colours indicate the amount of settleable particles: (blue is no particles (concentration  $ST1 = 0$ ) and red is the maximum amount of particles ( $ST1 = 1.0$ ). The white almost horizontal line gives the location of the water surface. The other white lines indicate where the horizontal velocity is zero. For example, for  $t = 300 \text{ s}$  the water in most of the tank flows to the left while just right of the internal weir near the bottom the water flows to the right (negative velocity).

#### 10 s

The incoming water causes a wave in the water which moves ahead of the incoming dirty water.

#### 60 s

The over the weir falling water creates an anti-clockwise turning eddy just right of the weir. Because of the settling of particles on the bottom, the concentrations diminish.

#### 180 s

When the water level in the tank (downstream of the internal weir) rises above the weir crest, the recirculation turns. Apparently during this turning the new incoming water is used in the growing eddy (recirculation zone), whilst a plume of the dirty water, which came in before, is pushed forward. Meanwhile the particles deposit on the bottom, so the concentration in the water drop.

#### 300 s

After 240 seconds the water reaches the crest of the external weir and starts to flow out. The recirculation zone grows and the plumes disappears almost completely.

#### 420, 600, 780 s

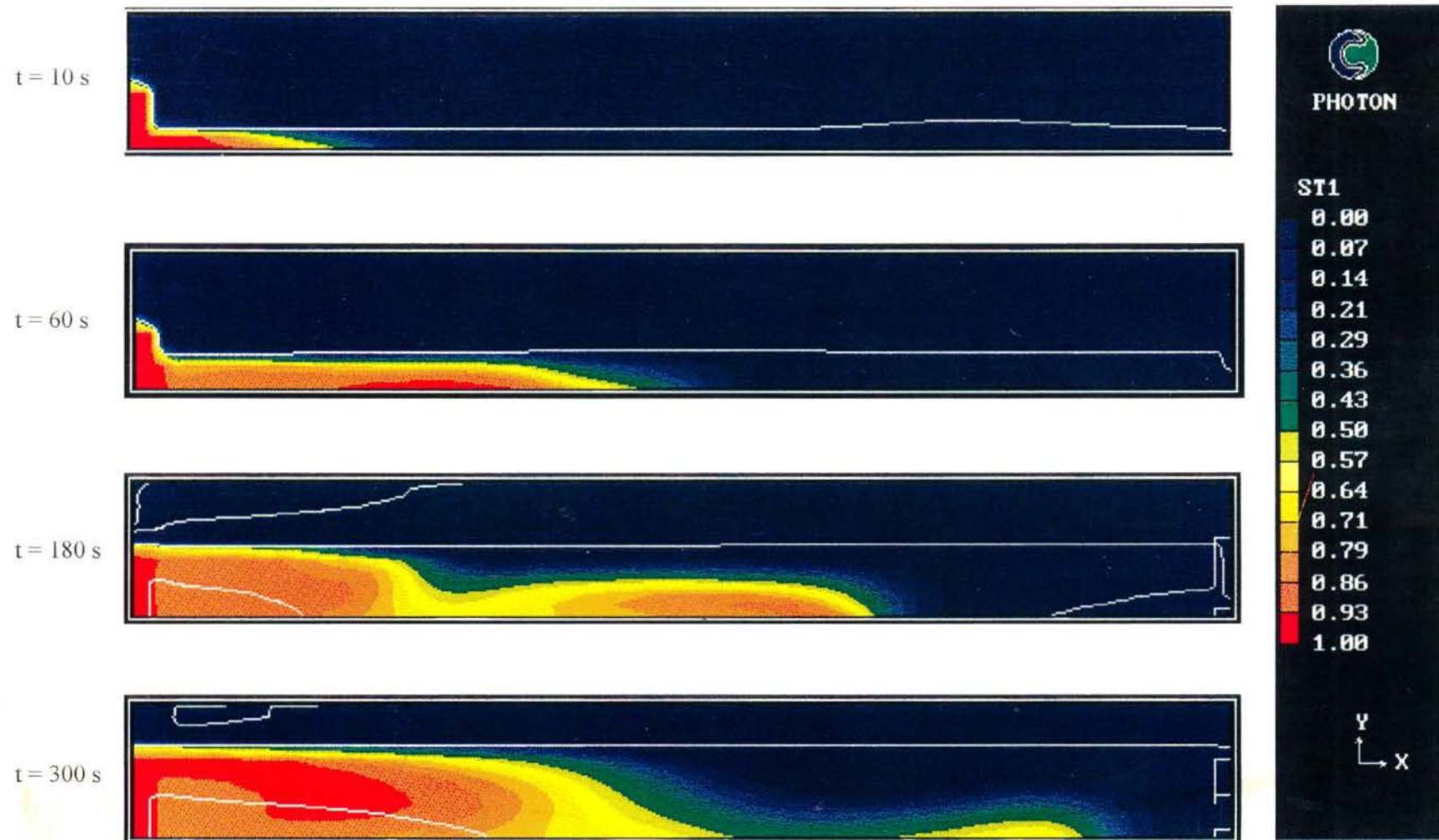
The recirculation zone grows to a final length of about 7.4 m. This is equal to  $6.2 * H_i$  or 37% of the length of the tank.

After 780 s (13 minutes) the flow situation hardly changes and the computations have been stopped. The concentration of particles in the outflowing water is then about 30%.

#### Computational time

The computational time for the simulation of these 13 minutes flow were considerable: 10 hours at a work-station. This is due to the high velocities occurring during the filling. In order to prevent divergence of the computation (and

# Filling of tank and settling of particles





# Filling of tank and settling of particles <sup>2</sup>



Figuur 4.3:

consequently useless results) in computations with a free water surface the Courant number has always and everywhere to be smaller than 1. The water falls over the weir into the tank with a velocity of 2.7 m/s. With a cell height of 0.2 m the time step then has to be smaller than 0.074 s. The computations have been started with a time step of 0.025 s. After the filling the time step was increased to 0.5 s.

In fact the water level hardly changes after the water level has risen above the external weir crest. To save computational time from that moment on a much faster rigid lid computation (with the rigid lid at the location of the water surface and the proper boundary conditions along this rigid lid) could be carried out.

#### 4.4.2 Particle diffusion

Only the diffusion of the momentum and not the diffusion of the particles is computed. The inevitable numerical diffusion causes the dispersion of the concentration. Without this numerical diffusion in the equilibrium situation a sharp line in the tank would indicate the border between clear and dirty water. The numerical diffusion does not influence the outcome significantly if it is much smaller than the real diffusion. Although this real diffusion has not been computed here, it can be estimated.

With the used fully upwind discretisation of the equilibrium equations the coefficient of the numerical diffusion is  $u \cdot DX/2 \cdot (1 + \sigma)$ , with  $\sigma = u \cdot DT/DX$ . In the equilibrium situation at the right of the recirculation zone the velocity is  $u = 0.05$  m/s. With a cell length (DX) of 0.2 m  $\sigma$  ( $u \cdot DT/DX$ ) equals 0.0125. Consequently the numerical diffusion coefficient equals 0.005 m<sup>2</sup>/s.

The real diffusion coefficient equals  $\nu_l/\sigma_l + \nu_t/\sigma_t$ .

$\nu_l$  = laminar viscosity =  $1.79 \cdot 10^{-6}$

$\sigma_l$  = laminar Prandtl-number = 0.5 to 1 (1 is chosen here)

$\nu_t$  = turbulent viscosity =  $1 \cdot 10^{-6}$  tot 0.2 (computed with PHOENICS)

$\sigma_t$  = turbulent Prandtl-number = 0.5 tot 1 (1 is chosen here)

In the equilibrium situation at the right of the recirculation zone the diffusion coefficient thus equals 0.003 m<sup>2</sup>/s. Consequently the numerical diffusion is important in comparison to the real diffusion. The numerical diffusion can be diminished by choosing a finer grid or an other numerical discretisation scheme.

The transport due to the numerical diffusion ( $u \cdot DX/2 \cdot (1 + \sigma) \cdot d^2c/dx^2$ ) is however still small compared to the convective transport ( $u \cdot dc/dx \cdot DY$ ).

#### 4.4.3 Bottom boundary condition for settleable solids

All the sediment reaching the bottom was assumed to deposit and was taken out of the model. No resuspension was taken into account. This is not realistic and will be replaced by a more realistic boundary condition in the future.

## 5 CONTINUATION OF RESEARCH

With the validated flow model the filling of a tank will in the future be investigated in more detail than in [Kluck, 1993-a], but evaluating different shapes of tanks will not be carried out extensively until the sedimentation is part of the model. Only the possibilities of the model to compute the flow in different flow situations will be tested. One example is the flow through the diffusor for which some measurements have been carried out (situation 5 [Kluck, 1994]).

The diffusion terms will be added to the new method to compute the particle distribution. In order to represent correctly the deposition and re-entrainment a boundary condition for the concentration near the bottom will have to be found. Furthermore this method will have to be tested in some flow situations.

Measure data to validate the sedimentation method is needed. Accurate measurements with sediment in real storm water sedimentation tanks are not available. The remaining time of this project is too short to set up and carry out a good measure program. Therefore, from literature measurements in scale models of storm water sedimentation tanks or similar flow conditions with similar sediment will be searched. There are some options:

- \* The municipality of Amsterdam is going to carry out measurements in a storm water sedimentation tank. Probably the results can be used to validate the model.
- \* At the university of Sheffield measurements in a storage tank have been carried out. In the prototype of this scale model the deposition of particles has to be minimized. The average flow field and the turbulent fluctuations have been measured accurately. The deposition of particles is measured. Possibly the flow through this experimental setup can be modelled and the computed deposition of particles can be compared with the measured deposition.
- \* The possibilities of setting up a measuring project in an available scale model of a storm water sedimentation tank (DHV-Milieu en Infrastructuur) are still being investigated. Possibly the deposition of sediment in this scale model can be monitored. Also the effect of varying the flow rate and the presence of a diffusor. These data can be used to validate the particle model.

Further useful measurements from literature have not yet been found. Many research projects deal with slow varying density currents in secondary clarifiers, which is quite different from the faster varying flow in storm water sedimentation tanks.

At the moment storm water sedimentation tanks are designed even without sufficient knowledge about the particles entering the tanks and which particles have to be retained. A project to investigate this is initiated at the Rotterdam waste water treatment plant 'De Dokhaven'. A relation between the settling velocity and certain pollution parameters is to be found with the method as presented in [Michelbach and Wöhrle, 1992]: During heavy rain samples of the incoming water (a mixture of waste water, rain and eroded sewer sediments) will be taken. By means of sedimentation, each sample will be split in a series of smaller samples. Each of these smaller samples represents a certain settling velocity. By analyzing these samples the required relations are to be found. The

results are possibly only valid for the sewer system of Rotterdam, but will give at least an indication for other systems.

With the final working total model (flow and sedimentation) the working of different shapes of tanks can be examined for time varying inflows. If the computational time to simulate one storm through a tank can be kept small enough, it will be possible to evaluate different designs for a range of storms. A given volume could be shaped in different ways: a cheap design, some designs made with now used standard restrictions such as Reynolds, Froude and Camp, etc.



## ANNEXES A: REFERENCES

Booij R., 1986, *Turbulentie in de waterloopkunde*, lecture notes b82, TUD, Delft.

CHAM, 1994, *POLIS: PHOENICS on line information system*, part of PHOENICS version 2.0, 1994.

Chen, Y.S. and Kim, S.W., 1987, *Computation of turbulent flows using an extended k-e turbulence closure model*, NASA CR-179204.

Kluck, J., 1992-a, *Onderzoek aan bergbezinktanks: Stand van zaken*, TUD, Delft.

Kluck J., 1992-b, *Een mathematisch model voor het hydraulische gedrag van bergbezinktanks*, TUD, Delft.

Kluck, J., 1993-a, *Het modelleren van een vrij wateroppervlak in bergbezinktanks*, TUD, Delft.

Kluck, J., 1993-b, *Modellering van de waterbeweging in bergbezinktanks met PHOENICS* TUD, Delft.

Kluck, J., 1994, *Modelling of flow and settling in storm water sedimentation tanks*, TUD, Delft.

Michelbach, S. and Wöhrle, C., 1992, *Settleable solids in a combined sewer system - measurements, quantity, characteristics*, Wat. Sci. Tech. Vol 25 no 8.

Rodi W., 1980, *Turbulence models and their application in hydraulics - a state of the art review*, University of Karlsruhe, , Karlsruhe.

Tropea C., 1982, *Die turbulente Stufenströmung in Flachkanälen und offenen Gerinnen*.

## ANNEXES B: Settleable solids subroutine for PHOENICS

Below a part of the GROUND.FOR file is given. The GROUND.FOR file is used by the PHOENICS-user to add own coding to the flow model.

The following part is called at the beginning of each time step.

```
C
C--- GROUP 19. Special calls to GROUND from EARTH
C
  19 GO TO (191,192,193,194,195,196,197,198,199,1910,1911),ISC
  191 CONTINUE
C * ----- SECTION 1 ---- Start of time step.
c lsg1 is true bij HOL berekening.
  if (.not.lsg1) return
  l0stold=l0f(c2)
  LOST=L0F(C1)
  do ix = 1,nx
  do iy = 1,ny
    ITEL=IY+NY*(IX-1)
    f(l0stold+ITEL)=F(LOST+ITEL)
  ENDDO
  ENDDO
  RETURN
```

The next part is called at the end of each time step.

```
C * ----- SECTION 8 ---- Finish of time step.
C STOFTRANSPORT
c computations with free surface
C IF (ISWEEP.lt.LSWEEP-1) RETURN
  LOU1=L0F(U1)
  LOV1=L0F(V1)
  LOST=L0F(C1)
  LOSTOLD=L0F(C2)
  LOVS=L0F(LBNAME('VS'))
  LOBRON=L0F(LBNAME('BRON'))
  LODEN1=L0F(DEN1)
  LODX=L0F(DXU2D)
  LODY=L0F(DYV2D)
  LOVFOL=L0F(LBNAME('VFOL'))
  LOVISL=L0F(VISL)
  LOAN = L0F(ANORTH)
  LOae = l0f(aeast)
  DO IX=ixf,ixl
  DO IY=iyf,iyl
    II=IY+NY*(IX-1)
    F(LOVS+II)=(2650-f(LODEN1+ii))/F(LODEN1+II)*9.81*rsg11*rsg11
+    /(18*f(LOVISL+ii))*(1+(1000.5-F(LODEN1+II))/10)
  ENDDO
  ENDDO
  DO III=1,20
  DO IX=ixf,ixl
  DO IY=iyf,iyl
    II=IY+NY*(IX-1)
    dy=F(LODY+II)
    if (ix.eq.1) then
      sflhor1=0.
      flhor3=0.
      sflhor4=MIN(0.,F(LOu1+II))*(F(LOST+II+ny))*F(LOAE+II)
      flhor2=Max(0.,F(LOu1+II))*F(LOAE+II)
    else
      sflhor1=MAX(0.,F(LOu1+II-ny))*(F(LOST+II-ny))*F(LOAE+II-NY)
      flhor3=Min(0.,F(LOu1+II-ny))*F(LOAE+II-NY)
      IF (IX.LT.Nx) then
        sflhor4=MIN(0.,F(LOu1+II))*(F(LOST+II+ny))*F(LOAE+II)
        flhor2=Max(0.,F(LOu1+II))*F(LOAE+II)
      ELSE
```

```

        sflhor4=0.
        flhor2=0.
    endif
ENDIF
dx=F(LDDX+II)
if (iy.eq.1) then
    SFLVER1=0.
    FLVER3=Min(0.,-F(LOVS+II)*F(LOAN+II))*RSG14
+   /(MAX(0.1,F(LOVFOL+II)))
    sFLVER4=Min(0.,F(LOV1+II)-F(LOVS+II))*F(LOST+II+1)
+   *F(LOAN+II)/(MAX(0.1,F(LOVFOL+II+1)))
    FLVER2=Max(0.,F(LOV1+II)-F(LOVS+II))*F(LOAN+II)
else
    SFLVER1=MAX(0.,F(LOV1+II-1)-F(LOVS+II-1))*F(LOST+II-1)
+   *F(LOAN+II)
    FLVER3=Min(0.,F(LOV1+II-1)-F(LOVS+II-1))*F(LOAN+II-1)
+   /(MAX(0.1,F(LOVFOL+II)))
    IF (IY.LT.NY) then
        SFLVER4=Min(0.,F(LOV1+II)-F(LOVS+II))*F(LOST+II+1)
+        *F(LOAN+II)/(MAX(0.1,F(LOVFOL+II+1)))
        FLVER2=Max(0.,F(LOV1+II)-F(LOVS+II))*F(LOAN+II-1)
    ELSE
        SFLVER4=0.
        flver2=0.
    endif
ENDIF
stold=(f(l0stold+II)*DX*DY/DT+F(LOBRON+II))
f(l0ST+II)=((sFLVER1-sFLVER4+sflhor1-sflhor4+STOLD)/
+   (flver2-flver3+flhor2-flhor3+DX*DY/DT))
ENDDO
ENDDO
ENDDO
RETURN

```